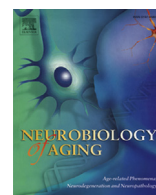




Contents lists available at ScienceDirect

## Neurobiology of Aging

journal homepage: [www.elsevier.com/locate/neuaging](http://www.elsevier.com/locate/neuaging)

# The resting perfusion pattern associates with functional decline in type 2 diabetes

Weiying Dai<sup>a,\*</sup>, Wenna Duan<sup>a</sup>, Freddy J. Alfaro<sup>b</sup>, Anna Gavrieli<sup>b</sup>, Fotini Kourtellis<sup>c</sup>, Vera Novak<sup>b</sup>

<sup>a</sup> Department of Computer Science, State University of New York at Binghamton, Binghamton, NY, USA

<sup>b</sup> Department of Neurology, Beth Israel Deaconess Medical Center, Harvard Medical School, Boston, MA, USA

<sup>c</sup> Department of Radiology, Beth Israel Deaconess Medical Center, Harvard Medical School, Boston, MA, USA

## ARTICLE INFO

## Article history:

Received 22 March 2017

Received in revised form 5 September 2017

Accepted 6 September 2017

## Keywords:

Type 2 diabetes mellitus

Cognitive impairment

Cerebral blood flow

Arterial spin labeling MRI

Voxel-based analyses

Insulin resistance

## ABSTRACT

We investigated the relationships between cerebral blood flow (CBF), cognitive, and mobility decline in type 2 diabetes mellitus (T2DM) over a 2-year period. Seventy-three participants (41 T2DM and 32 controls) were evaluated using volumetric CBF with arterial spin labeling perfusion magnetic resonance imaging at baseline and at the 2-year follow-up. Regions with significant CBF differences between T2DM participants and controls at baseline were detected using voxel-wise analysis. Correlation analysis was performed to investigate the association between regional CBF and cognitive or mobility performance over the 2-year span. Compared to controls, participants with T2DM had decreased CBF in the resting-state default mode, visual, and cerebellum networks. Greater decrease in longitudinal CBF values at these regions over a 2-year span was associated with worse gait, memory and executive functions, and higher baseline insulin resistance and worse baseline cognitive performance. In T2DM, impairment of resting regional perfusion is closely related to worse cognitive and mobility performance. Insulin resistance may further contribute to regional perfusion deficit in T2DM.

© 2017 Elsevier Inc. All rights reserved.

## 1. Introduction

Type 2 diabetes mellitus (T2DM) is associated with altered cerebral vasoreactivity (Chung et al., 2015; Last et al., 2007; Novak et al., 2011), cerebral atrophy (Franke et al., 2013; Novak et al., 2011; van Elderen et al., 2010), cognitive impairment (Chung et al., 2015; Wong et al., 2014), and functional decline (Chung et al., 2015). T2DM-related endothelial dysfunction secondary to a chronic state of hyperglycemia, inflammation, and insulin resistance (Brownlee, 2005; Kim et al., 2006; Starr et al., 2003) has been associated with alterations in the blood-brain barrier (Mogi and Horiuchi, 2011; Starr et al., 2003), neuronal damage (Umegaki, 2014), and arterial stiffness (Zhou et al., 2014), thus negatively affecting cerebral metabolism and cerebral blood flow (CBF) (Roberts et al., 2014).

Arterial spin labeling (ASL) is a functional magnetic resonance imaging (MRI) technique capable of quantifying regional CBF, among the several neuroimaging techniques. ASL is a noninvasive technique that magnetically labels the water in the blood vessels

(Detre et al., 1992; Williams et al., 1992). ASL has been recently used to evaluate CBF in T2DM patients; however, the reports are contradictory. Some studies found that resting CBF is similar between T2DM patients and controls (Novak et al., 2011; Rusinek et al., 2015; Tiehuis et al., 2008), whereas others reported reduced CBF in patients with T2DM (Last et al., 2007; Nagamachi et al., 1994; Novak et al., 2006; Xia et al., 2015). The cross-sectional design of these studies, however, did not allow to investigate the association between T2DM and changes in brain perfusion or structure and cognitive or mobility functions over time. Pseudo-continuous ASL (PCASL), with great labeling efficiency (Dai et al., 2008; Wu et al., 2007) and recommended for clinical applications (Alsop et al., 2014), was adopted for the measurement of whole-brain CBF maps. Moreover, PCASL has been shown to have excellent test-retest reliability for both young and elderly subjects (Xu et al., 2010) and hence, can serve as a useful technique even for longitudinal studies.

In the present study, we used ASL CBF imaging to determine the effect of T2DM on CBF at baseline and the relationship between CBF and functional outcomes (cognition and gait) at baseline and after the 2-year follow-up. We hypothesized that (1) T2DM is associated with altered resting perfusion patterns and (2) impaired CBF is associated with alterations in cognitive function and gait.

\* Corresponding author at: Department of Computer Science, Binghamton University, N-14, Engineering Building, Binghamton, NY 13902, USA. Tel.: +1 607 777 4859; fax: +1 607 777 4729.

E-mail address: [wldai@binghamton.edu](mailto:wldai@binghamton.edu) (W. Dai).

## 2. Methods

The current work is an analysis from our prospective study on cerebrovascular disease in elderly with T2DM. The study was conducted at the Syncope and Falls in the Elderly laboratory, Clinical Research Center, and MRI Center of Beth Israel Deaconess Medical Center (BIDMC) between August 2009 and July 2013. Participants were recruited from the greater Boston area using community advertisement. They were assigned to either the T2DM group or the nondiabetic control group.

### 2.1. Participants

A hundred thirty-one participants, 50–85 years, were enrolled in this 2-year study. All participants signed written informed consent approved by the Committee on Clinical Investigations of BIDMC. Of 131 participants, 73 participants, 41 T2DM and 32 nondiabetic controls were eligible and included in baseline analysis, according to the inclusion criteria of the study. Of those, 42 participants, 19 T2DM and 23 nondiabetic controls, who completed the 2-year follow-up were included in the follow-up analyses.

Inclusion criteria for the T2DM group were men and postmenopausal women aged 50–85 years, diagnosed with T2DM, and treated with oral agents and/or insulin for more than 5 years, with hypertension (blood pressure [BP]  $\geq 140/90$  mm Hg and/or treated for hypertension) or without hypertension (BP  $< 140/90$  mm Hg and no medical history of hypertension). Inclusion criteria for the control group were men and postmenopausal women with normal fasting blood glucose and glycated hemoglobin A1c (HbA1c) matched with the diabetes group by age  $\pm 5$  years, gender, and presence of hypertension. Exclusion criteria for both groups were type I diabetes mellitus, any unstable or acute medical condition, myocardial infarction or major surgery within 6 months, history of a major stroke, carotid stenosis  $> 50\%$  by medical history, Doppler ultrasound or by magnetic resonance angiography, hemodynamically significant vascular disease, arrhythmias, liver or renal failure or transplant, severe hypertension (systolic BP  $> 200$  and/or diastolic BP  $> 110$  mm Hg or subjects taking 3 or more antihypertensive medications), seizure disorders, malignant tumors, current recreational drug or alcohol abuse, active smoking, morbid obesity (body mass index  $> 40$ ), dementia (by history), or Mini-Mental State Examination (MMSE) score ( $\leq 24$ ). MRI exclusion criteria included incompatible metal implants, pacemakers, and claustrophobia.

Reasons for exclusion from baseline analyses included withdrew consent ( $n = 11$ ), lost to follow-up ( $n = 10$ ), smoking ( $n = 1$ ), arrhythmias ( $n = 4$ ), cancer ( $n = 2$ ), MMSE score  $\leq 24$  ( $n = 3$ ), stroke/transient ischemic attack ( $n = 2$ ), heart failure ( $n = 1$ ), MRI exclusion criteria ( $n = 1$ ), renal failure ( $n = 1$ ), T2DM  $< 5$  years ( $n = 3$ ), poor glycemic and/or hypertension control ( $n = 7$ ), undetermined neurologic disorder ( $n = 2$ ), adverse event ( $n = 1$ ), and incomplete data sets ( $n = 9$ ). Reasons for exclusion after 2-year follow-up period included withdrew consent ( $n = 5$ ), lost to follow-up ( $n = 25$ ), and new diagnosis of dementia ( $n = 1$ ).

### 2.2. Experimental protocol

Screening visit included medical history review, completion of autonomic function questionnaires, physical and neurological evaluation, electrocardiogram, and fasting laboratory measurements.

After enrollment, participants came for an inpatient 2-day baseline visit at the BIDMC Clinical Research Center. On day 1, participants had vital signs and anthropometric measurements taken, including height and weight, and a cognitive assessment

battery testing. On day 2, a fasting blood draw was obtained, a cognitive assessment battery testing and walking test were completed, and MRI scans were performed. The same protocol was completed at the 2-year follow-up visit.

### 2.3. Cognitive assessment

The cognitive assessment battery that was used is a standard battery of cognitive tests that evaluate specific domains of cognition and daily living activities. It consists of measures of learning and memory (Hopkins Verbal Learning Test-Revised [HVLT-R] [Shapiro et al., 1999] and MMSE [Folstein et al., 1975]), measures of executive function (verbal fluency [VF] [Benton and Hamsher, 1989], Trail Making [Pugh et al., 2003], clock drawing [CD] [Grande et al., 2005]), and measures of attention (Digit Span [DS] [Wechsler, 1987]). HVLT-R includes a total recall (HVLT: total recall, total number of list items learned across trials), delayed recall (HVLT: delayed recall, total number of list items recalled after the delay), retention (HVLT: retention, percentage of items from HVLT: total recall that are subsequently recalled on HVLT: delayed recall), and Recognition Discrimination Index (HVLT: RDI, number of list items correctly identified among non-list items). MMSE assesses cognitive impairment. VF assesses phonemic and semantic fluency tasks. The phonemic fluency task requires the participant to generate as many words as possible beginning with a given letter (e.g., “S”) for 1 minute. The semantic fluency task requires the participant to generate items of a given semantic category (e.g., animals) for 1 minute. Dependent variables for the fluency measures include the number of items generated for all 3 phonemic trials (e.g., F, A, S; VF FAS total) and the number of items generated for the semantic task (e.g., animals; VF: animals). A composite executive score was calculated from all 3 measures of executive functions (VF, Trail Making, and CD). DS assesses immediate memory/attention.

### 2.4. Gait assessment

Participants completed two 6-minute walking tests on a 75-m course of an  $80 \times 4$  m indoor hallway. For the first test, participants were instructed to walk for 6 minutes at their usual and comfortable pace (normal walk), whereas for the second dual-task (DT) test, they were asked to perform the same while counting backwards. The time taken to complete each 75-m length and the total distance walked were recorded. No assistive devices were used for ambulation. The rate of perceived exertion (RPE) before and after each walking test was self-rated on a 10-point scale. Gait speed was calculated by dividing distance (m) by time (second).

### 2.5. Blood samples analysis

Serum/plasma glucose, insulin panels, and hematocrit were measured at Lab Corp (Laboratory Corporation of America Holdings, Burlington, NC, USA). The homeostatic model assessment of insulin resistance (HOMA-IR) was calculated as the product of fasting glucose (mg/dL) times insulin levels (mU/L) divided by 405 [Matthews et al., 1985].

### 2.6. MRI acquisition

All participants (73 participants at baseline and 42 participants at the 2-year follow-up) were scanned at the same 3-Tesla, GE HDxt scanner using a receive-only 8-channel head array coil and a body transmit coil. ASL images were obtained using the PCASL (Dai et al., 2008) with a 1.5 seconds labeling and 1.5 seconds post-labeling delay. Additional reference images for  $M_0$  values were obtained for absolute perfusion quantification. All ASL and reference images

were acquired with a 3-dimensional stack of spirals rapid acquisition with refocused echoes imaging sequence (repetition time = 5 seconds, field of view =  $24 \times 24$  cm, slice thickness = 4 mm, matrix size:  $128 \times 128 \times 40$ , bandwidth = 62.5 kHz). T1 anatomical images were acquired with a 3-dimensional magnetization-prepared rapid acquisition gradient echo sequence (repetition time = 7.9 ms, echo time = 3.2 ms, flip angle = 158, bandwidth = 32 kHz, coronal acquisition plane field of view =  $24 \times 19$  cm, in-plane resolution = 0.94 mm, slices = 1.4 mm, preparation time with repeated saturation at the beginning of the preparation period = 1100 ms, and adiabatic inversion pulse before imaging = 500 ms). An MRI scanner upgrade was performed between the baseline and 2-year follow-up scans, and the global signals may be altered between the scans. Therefore, we chose to present the relative CBF for the longitudinal analysis to reduce the effects of global signal change between 2 years.

### 2.7. Image processing

Quantitative CBF images were calculated for each participant as previously described (Alsop and Detre, 1996; Buxton et al., 1998; Wang et al., 2002). CBF maps were normalized to the a priori gray matter (GM) template using the SPM8 software package (<http://www.fil.ion.ucl.ac.uk/spm/>). T1 anatomical images served as intermediate images for CBF image normalization as they allow better alignment with the template. They were segmented by the “new segment” algorithm (Ashburner and Friston, 2005; Klein et al., 2009), which output GM images as well as other images in the original image space. Subtraction images (between label and control) from PCASL acquisition were coregistered to the GM images from the segmentation, and then the GM images were normalized to the GM template. The combined warping parameters from the coregistration and normalization were used to warp the quantitative CBF maps from each subject to the template space. Quantitative CBF maps were smoothed using a gaussian kernel with full-width at half maximum of 8 mm. Global CBF was calculated as the average of the CBF values on the whole brain mask.

To control for the effects of potential differences in tissue volume between the 2 groups that could account for differences of CBF, the GM probability map for each participant was generated using T1 anatomical images from the segmentation of SPM8. The binary map of GM probability map (assign 1/0 to the voxels with GM probability greater/lower than 0.2) was transformed to the standard GM template using SPM spatial normalization with volume-preserving transformation. Total volume of GM was calculated and used as a covariate of CBF analysis for GM volume correction.

### 2.8. Statistical analysis

Demographic and neuropsychological data were analyzed with MATLAB, version R2015a. All tests were 2-tailed, and significance was set for  $p < 0.05$ . Normality was assessed with Shapiro-Wilk test. Differences in demographic and neuropsychological characteristics at baseline and 2-year follow-up between the T2DM patients and the controls were compared using either 2-sample  $t$  tests or Mann-Whitney nonparametric  $U$  tests for continuous variables and  $\chi^2$  test for categorical variables.

#### 2.8.1. Global CBF and CBF maps at baseline and 2-year follow-up

Global CBF between the 2 groups was initially compared at baseline using 2-sample  $t$  test. Given that hematocrit and gender are important predictors of CBF (Henriksen et al., 2013, 2014; Liu et al., 2012), and hematocrit is significantly different between the 2 genders ( $p \leq 0.001$ , in the present study), Pearson correlation was performed between each variable (hematocrit or gender) and CBF

to determine which one is the most sensitive predictor of CBF. Hematocrit ( $r = -0.39$ ,  $p \leq 0.001$ ) but not gender ( $r = 0.18$ ,  $p = 0.14$ ) was negatively correlated with CBF, thus hematocrit was used as a confounder in the subsequent analysis. Multiple linear regression analysis was performed with CBF as the dependent variable, group (T2DM/Control) as the independent variable, and age, hematocrit, and hypertension (presence/no presence) as confounding variables.

To examine CBF differences between the 2 groups across the whole brain volume, CBF map was modeled as a multiple linear regression on a voxel-by-voxel basis using SPM8. Age, hematocrit, and hypertension were included as covariates. The voxel-level significance threshold was set for  $p < 0.005$ , whereas the cluster-level threshold was set for  $p < 0.05$  to minimize any false positive findings because of the multiple comparisons.

Owing to the potentially increased family-wise error (FWE) rates from the SPM cluster-level analysis (Eklund et al., 2016; Woo et al., 2014), we verified the statistical results using Statistical nonParametric Mapping (SnPM, <http://www.sph.umich.edu/ni-stat/SnPM/>). The nonparametric approach was shown to be robust with the nominated false positive rate of 5% (Eklund et al., 2016). In the SnPM analysis, the CBF map was modeled as a multiple linear regression on a voxel-by-voxel basis. Age, hematocrit, and hypertension were included as covariates same as those in the SPM analysis. One-thousand random permutations were performed on the disease state (either T2DM or control). For each permutation, a voxel-level  $p$ -value threshold of 0.005 (same as SPM analysis) was chosen to define clusters first, and then the largest suprathreshold cluster size was calculated. Largest cluster sizes from all 1000 permutations were used to calculate the empirical distribution to correct for multiple comparisons among voxels. The cutoff cluster size with FWE of 5% was derived. The T2DM-affected regions were used for further region-based analysis. Based on the T2DM-affected regions at baseline, post hoc brain network-based analysis was also performed to identify the involvement of brain networks in T2DM. CBF value at each identified brain network was calculated as the mean CBF over the corresponding brain network mask. The brain network masks were generated from our recent ASL resting-state network study (Dai et al., 2016).

Global CBF values and CBF maps between the T2DM group and the control group were compared at the 2-year follow-up using the same approach as described at baseline. Regional and network CBF values at the regions and networks affected by T2DM (derived from baseline) were calculated at the follow-up and compared using 2-sample  $t$  tests and multiple linear regression with the same confounding variables as in the global CBF comparisons at baseline.

#### 2.8.2. Post hoc correlation analysis of regional and network CBF at baseline

To investigate the relationship between CBF in the brain regions and networks affected by T2DM and cognitive and mobility performance, post hoc correlation analysis was performed. The partial correlation coefficients between the regional CBF values and cognitive or mobility performance scores were examined with age, hematocrit, and hypertension, being used as covariates. Because the difference in GM volume between T2DM and control groups could potentially account for the CBF differences between the 2 groups, GM volume was further included in the partial correlation analysis as an additional covariate.

#### 2.8.3. Longitudinal change of global CBF and CBF maps over a 2-year period

Longitudinal change of global CBF was compared between the T2DM and control groups using a multiple linear regression with the same confounding variables as in the global CBF comparison at baseline. Longitudinal change of CBF maps was also compared

between the 2 groups using the same SPM8 voxel-by-voxel analysis as in the comparison of CBF maps at baseline. For the longitudinal change of CBF maps, we used the relative CBF maps (calculated as the ratio of CBF maps to the associated global CBF value) at baseline and 2-year follow-up to reduce the effect of potentially altered global CBF over a 2-year period. Longitudinal regional and network CBF change at the T2DM-affected regions and networks (derived from the baseline study) was also compared using the same tests as in the baseline regional CBF comparison. The relative regional CBF values (regional CBF values divided by the corresponding global CBF values) were also used in the calculation of longitudinal regional CBF change.

#### 2.8.4. Correlation of longitudinal CBF change with longitudinal variable change/baseline variable

The longitudinal correlation analysis was performed only for the T2DM-affected regions and networks. To investigate whether the longitudinal CBF change is related to the longitudinal change of cognitive and mobility performance, post hoc correlation analysis was performed. Partial correlation coefficients were calculated between CBF change and the baseline variables (including cognitive, mobility, and disease severity variables) to investigate which baseline variables can predict the longitudinal CBF change. Age, hematocrit, hypertension, GM volume, and education years were used as covariates. Education was included as an additional covariate because it was significantly different between the T2DM and control groups at 2-year follow-up ( $p = 0.012$ ).

### 3. Results

Table 1 summarizes participants' demographic and clinical characteristics, gait results, and cognitive scores at baseline and at

the 2-year follow-up. At baseline, no differences between age, gender, education, and hematocrit values were found between the 2 groups. T2DM group had higher prevalence of hypertension ( $p \leq 0.001$ ), body mass index ( $p = 0.007$ ), fasting glucose ( $p \leq 0.001$ ), HbA1c ( $p \leq 0.001$ ), insulin level ( $p = 0.003$ ), and HOMA-IR ( $p \leq 0.001$ ) compared to controls. Furthermore, participants with T2DM had worse performance on learning, memory, executive, attention, and mobility functions, including HVLT: total recall, HVLT: delayed recall, HVLT: RDI, VF: FAS total, VF: animal, CD, DS, composite executive score, gait speed (Normal), and gait speed (DT) ( $p < 0.05$ ), as compared to controls. Similar values between groups were found for MMSE, HVLT: retention, Trail Making, RPE before gait (Normal), RPE after gait (Normal), RPE before gait (DT), and RPE after gait (DT).

At the 2-year follow-up, the significant differences between the T2DM and control groups remained similar in demographics, clinical characteristics, gait results and cognitive scores. The markedly reduced number of participants rendered gait speed (DT) and Composite Executive Score results insignificant, while the years of education became significant.

#### 3.1. Global CBF at baseline

At baseline, the T2DM group had lower global CBF ( $29.83 \pm 9.78$  mL/100 g/min) as compared to controls ( $36.91 \pm 11.77$  mL/100 g/min), after adjusting for age, hematocrit, and hypertension diagnosis (yes/no) ( $p = 0.027$ ). Greater global CBF was associated with the presence of hypertension ( $r = 0.26$ ,  $p = 0.028$ ) and lower hematocrit levels ( $r = -0.43$ ,  $p = 0.0001$ ), but only marginally associated with younger age ( $r = -0.21$ ,  $p = 0.086$ ). The difference between the 2 groups was not observed on the unadjusted 2-sample  $t$  test comparison.

**Table 1**  
Demographic, clinical ratings, postural control, and cognitive scores at baseline and follow-up

Characteristic	Baseline			2-y Follow-up		
	T2DM (n = 41)	Controls (n = 32)	p value	T2DM (n = 19)	Controls (n = 23)	p value
Age (y)	65.51 $\pm$ 8.30	67.28 $\pm$ 10.08	NS	66.94 $\pm$ 8.18	67.09 $\pm$ 9.29	NS
Gender (females, N, %)	22 (54)	16 (50)	NS	12 (63)	12 (63)	NS
Education (y)	15.35 $\pm$ 3.78	16.05 $\pm$ 2.98	NS	14.03 $\pm$ 2.93	16.35 $\pm$ 2.81	0.012
Hematocrit (%)	38.83 $\pm$ 3.70	39.54 $\pm$ 3.89	NS	38.58 $\pm$ 3.21	38.71 $\pm$ 3.56	NS
Hypertension (N, %)	32 (78%)	7 (22%)	$\leq 0.001$	15 (79%)	5 (22%)	$\leq 0.001$
Diabetes duration (y)	9.93 $\pm$ 7.91	—	—	9.63 $\pm$ 6.91	—	—
BMI (kg/m <sup>2</sup> )	29.12 $\pm$ 6.77	25.17 $\pm$ 6.68	0.007	29.46 $\pm$ 5.43	24.05 $\pm$ 3.08	$\leq 0.001$
Insulin ( $\mu$ U/mL)	13.61 $\pm$ 13.30	6.26 $\pm$ 3.77	0.003	15.19 $\pm$ 17.55	6.06 $\pm$ 4.30	0.020
Fasting glucose (mg/dL)	119.70 $\pm$ 36.78	89.94 $\pm$ 10.22	$\leq 0.001$	112.69 $\pm$ 31.81	91.59 $\pm$ 8.92	0.005
HOMA-IR <sup>a</sup>	3.87 $\pm$ 3.42	1.40 $\pm$ 0.83	$\leq 0.001$	4.35 $\pm$ 4.67	1.33 $\pm$ 0.92	$\leq 0.001$
HbA1c (%)	7.34 $\pm$ 1.25	5.72 $\pm$ 0.30	$\leq 0.001$	7.82 $\pm$ 1.79	5.64 $\pm$ 0.33	$\leq 0.001$
Gait speed (normal) (m/s)	1.03 $\pm$ 0.15	1.16 $\pm$ 0.13	$\leq 0.001$	1.04 $\pm$ 0.14	1.18 $\pm$ 0.13	0.004
Gait speed (DT) (m/s)	0.92 $\pm$ 0.19	1.01 $\pm$ 0.19	0.049	0.97 $\pm$ 0.19	1.02 $\pm$ 0.21	NS
Gait (normal) RPE start	0.89 $\pm$ 1.56	0.28 $\pm$ 0.63	NS	0.58 $\pm$ 1.02	0.22 $\pm$ 0.42	NS
Gait (normal) RPE end	2.53 $\pm$ 2.02	1.81 $\pm$ 1.35	NS	2.21 $\pm$ 1.55	1.64 $\pm$ 1.22	NS
Gait (DT) RPE start	1.54 $\pm$ 1.88	0.55 $\pm$ 0.74	NS	1.06 $\pm$ 1.26	0.43 $\pm$ 0.68	NS
Gait (DT) RPE end	2.68 $\pm$ 2.00	2.33 $\pm$ 1.52	NS	2.84 $\pm$ 2.14	2.36 $\pm$ 1.56	NS
MMSE	28.59 $\pm$ 1.52	28.94 $\pm$ 1.56	NS	28.76 $\pm$ 1.35	28.83 $\pm$ 1.70	NS
HVLT: total recall	12.61 $\pm$ 13.04	30.40 $\pm$ 5.12	$\leq 0.001$	24.26 $\pm$ 6.07	27.96 $\pm$ 5.50	0.045
HVLT: delayed recall	43.03 $\pm$ 12.98	52.16 $\pm$ 10.86	0.002	42.47 $\pm$ 15.42	53.48 $\pm$ 11.70	0.012
HVLT: retention	81.87 $\pm$ 16.79	87.20 $\pm$ 16.66	NS	79.34 $\pm$ 17.95	84.63 $\pm$ 15.90	NS
HVLT: RDI	44.17 $\pm$ 12.28	50.79 $\pm$ 8.38	0.023	42.79 $\pm$ 13.29	50.52 $\pm$ 10.69	0.043
VF: FAS total	35.80 $\pm$ 10.79	45.38 $\pm$ 12.25	$\leq 0.001$	38.32 $\pm$ 13.47	49.57 $\pm$ 12.79	0.009
VF: animal	4.39 $\pm$ 1.38	9.72 $\pm$ 3.14	$\leq 0.001$	8.37 $\pm$ 3.30	11.48 $\pm$ 3.22	0.004
Trail Making	47.92 $\pm$ 11.37	50.60 $\pm$ 9.29	NS	50.89 $\pm$ 12.38	49.13 $\pm$ 8.44	NS
Clock drawing	6.71 $\pm$ 1.29	7.31 $\pm$ 0.82	0.027	6.68 $\pm$ 1.11	7.43 $\pm$ 0.73	0.016
Digit Span	50.05 $\pm$ 10.37	57.54 $\pm$ 12.10	0.008	47.83 $\pm$ 10.67	57.70 $\pm$ 8.90	0.004
Composite executive score	47.13 $\pm$ 8.09	51.87 $\pm$ 7.54	0.007	50.39 $\pm$ 8.51	51.33 $\pm$ 7.37	NS

Key: BMI, body mass index; DT, dual task; HbA1c, hemoglobin A1C; HOMA-IR, homeostatic model assessment of insulin resistance; HVLT, Hopkins Verbal Learning Test (Shapiro et al., 1999); MMSE, Mini-Mental State Examination; RDI, recognition discrimination index; RPE, rate of perceived exertion; T2DM, type 2 diabetes mellitus; VF, verbal fluency.

<sup>a</sup> HOMA-IR was derived to index insulin resistance by the homeostasis model (Matthews et al., 1985).

### 3.2. CBF maps at baseline

Compared to controls, T2DM patients had significantly lower CBF using SPM analysis after adjusting for age, hematocrit, and hypertension in 2 clusters: 1 large posterior cluster primarily in the occipital, cerebellum, posterior cingulate, precuneus, thalamus, parietotemporal, basal ganglia regions, and 1 anterior cluster in the ventromedial, ventrolateral, and orbitofrontal regions (Fig. 1A and B). Cluster statistics of the 2 clusters are shown in Table 2 with anatomical regions containing more than 1% of each cluster size or more than 30% of the entire anatomical regions listed. The cutoff cluster size with FWE of 5% from SnPM was 834 voxels. The posterior and anterior cluster sizes (Table 2) exceeded the cutoff cluster size threshold, supporting the CBF

deficits of T2DM at the posterior and anterior clusters derived from SPM analysis. The posterior cluster was in the posterior regions of default mode network (DMN), medial visual, and cerebellum networks (Fig. 1C), and the anterior cluster was located close to but not exactly in the prefrontal region of the DMN (Fig. 1D). CBF maps were significantly correlated with age, hematocrit, and hypertension (Fig. 2). Older participants showed significantly decreased CBF in the prefrontal regions (Fig. 2A). Higher hematocrit was correlated with significantly decreased CBF in extensive areas covering almost all cerebrum, including all frontal, parietal, occipital, and temporal regions (Fig. 2B). Hypertensive participants showed significantly increased CBF in the posterior cingulate, anterior cingulate, and prefrontal regions (Fig. 2C).

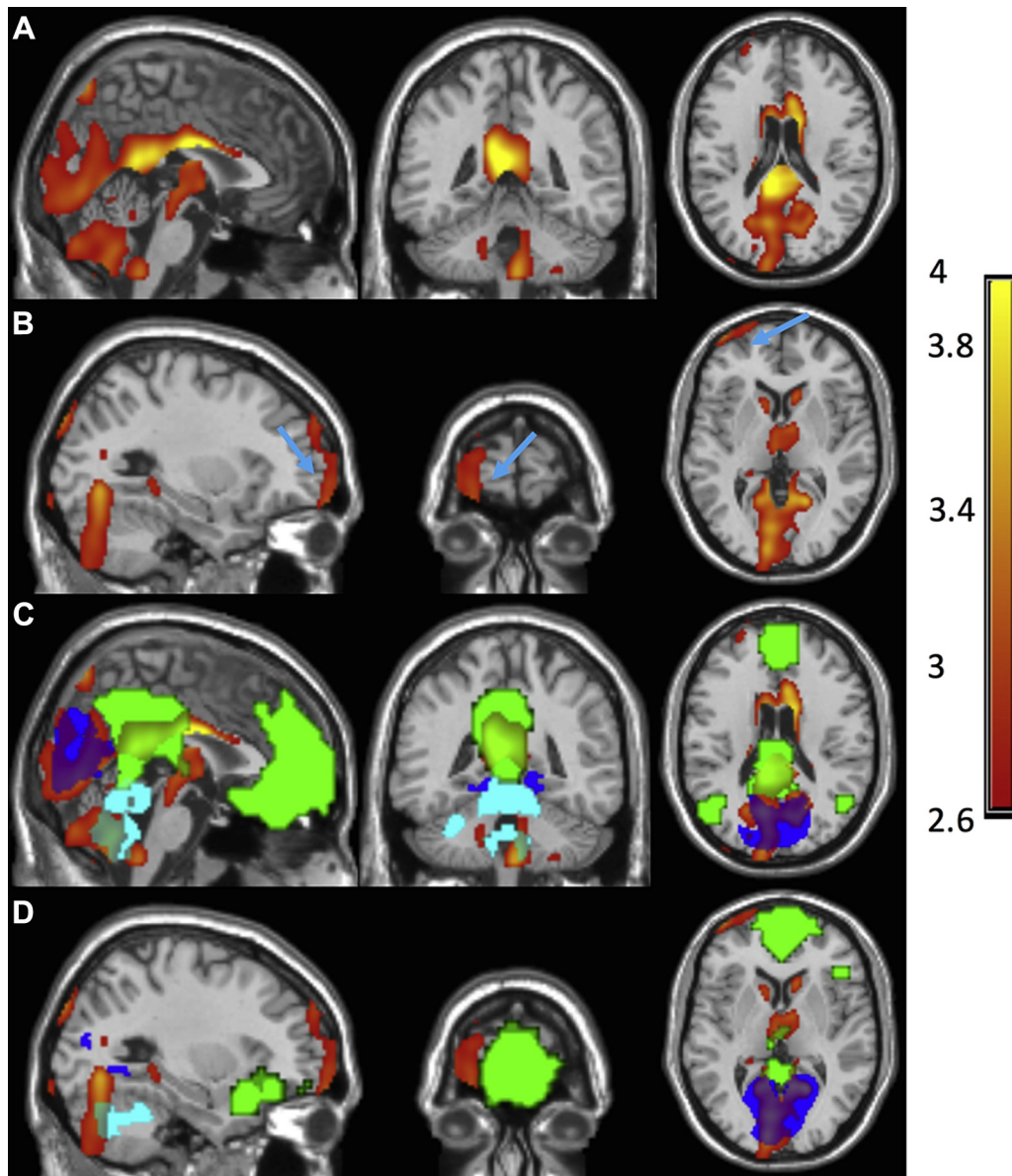


**Fig. 1.** Compared with controls, T2DM patients exhibited significantly reduced cerebral blood flow in (A) a posterior cluster, including occipital, cerebellum, posterior cingulate, precuneus, cuneus, thalamus, basal ganglia regions, and (B) an anterior cluster (pointed by light blue arrows), including the ventromedial, ventrolateral, and orbitofrontal regions. Cerebrospinal fluid was masked out from the clusters for better visibility. The posterior cluster exhibited (C) large overlap with the visual network (in blue color), cerebellum network (in cyan color), and the posterior part of the default mode network (in green color), while the anterior cluster was (D) close to (but not exactly in) the anterior part of the default mode network (in green color). The overlaps between the clusters (posterior cluster in (A) and anterior cluster in (B)) and the brain networks can be seen through the colored brain networks. (For interpretation of the references to color in this figure legend, the reader is referred to the Web version of this article.)

**Table 2**  
Clusters with significant CBF decrease in T2DM relative to age-matched controls

	N voxels	Peak-t	Peak-t Montreal Neurological Institute coordinates	Anatomical locations	%Cluster	%Region
Posterior cluster	32,240	4.63	−2, −8, 24	Cerebellum		
				Cerebellum_Crus1_R	4.61	56.16
				Cerebellum_Crus1_L	2.05	25.39
				Cerebellum_Crus2_R	4.63	70.48
				Cerebellum_Crus2_L	2.68	45.62
				Cerebellum_4_5_R	0.92	34.26
				Cerebellum_6_R	3.68	66.07
				Cerebellum_6_L	1.20	22.90
				Cerebellum_7b_R	1.17	70.60
				Cerebellum_7b_L	0.72	39.83
				Cerebellum_8_R	4.18	58.41
				Cerebellum_9_R	1.72	68.92
				Vermis_4_5	1.16	56.39
				Vermis_6	0.41	35.58
				Vermis_7	0.31	52.06
				Vermis_8	0.59	77.78
				Vermis_9	0.43	80.46
				Vermis_10	0.11	31.25
				Basal ganglia		
				Caudate_R	1.40	45.47
				Caudate_L	0.97	32.43
				Thalamus_R	1.44	43.80
				Thalamus_L	1.32	38.82
				Occipital lobe		
				Calcarine_R (visual)	2.40	41.64
				Calcarine_L (visual)	6.18	88.22
				Cuneus_R	0.93	31.00
				Cuneus_L	3.91	82.63
				Fusiform_L	1.28	17.84
				Lingual_R	4.22	59.09
				Lingual_L	3.61	55.56
				Occipital_Sup_L	2.33	54.90
				Limbic system		
				Cingulum_Post_R	0.85	82.09
				Cingulum_Post_L	1.37	95.46
				Parietal lobe		
				Precuneus_R	1.59	15.71
				Precuneus_L	3.08	28.17
Anterior cluster	1068	3.78	−44, 60, −10	Frontal Lobe		
				Frontal_Sup_L	17.51	5.20
				Frontal_Inf_Orb_L	1.40	0.89
				Frontal_Mid_L	4.49	0.99
				Frontal_Mid_Orb_L	12.55	15.09
				Frontal_Sup_Orb_L	2.25	2.49

%Cluster indicates the percentage of each cluster that falls within the defined region and %Region indicates the percentage of each defined region that falls within the cluster. The listed anatomical regions are either "%Cluster" >1% or "%Region" >30%.

### 3.3. Post hoc correlation analysis of regional and network CBF at baseline

Post hoc correlation analysis for all participants showed significant correlation between CBF and plasma insulin, HOMA-IR, gait speed, and VF performance after correcting for age, hematocrit, and hypertension. At the posterior cluster, an increase of CBF was associated with lower insulin levels ( $r = -0.35$ ,  $p = 0.0026$ ) and HOMA-IR ( $r = -0.35$ ,  $p = 0.0036$ ), higher gait speed (DT) ( $r = 0.40$ ,  $p = 0.0013$ ), and higher VF: animal score ( $r = 0.43$ ,  $p = 0.0002$ ). At the anterior cluster, an increase of CBF was associated with lower insulin levels ( $r = -0.28$ ,  $p = 0.019$ ), lower HOMA-IR ( $r = -0.30$ ,  $p = 0.011$ ), higher gait speed (DT) ( $r = 0.26$ ,  $p = 0.040$ ), and higher VF: animal score ( $r = 0.44$ ,  $p = 0.0002$ ). No significant associations were observed for the other variables reflecting T2DM severity (fasting glucose and HbA1c), cognitive performance (MMSE, HVLT-R, VF: FAS total, and DS), and gait measures.

The post hoc correlation analysis for the whole cohort was further corrected for GM volume. With the additional correction, the posterior cluster remained negatively associated with insulin levels ( $r = -0.32$ ,  $p = 0.0077$ ) and HOMA-IR ( $r = -0.30$ ,  $p = 0.012$ ),

and positively associated with gait speed (DT) ( $r = 0.38$ ,  $p = 0.0025$ ) (Fig. 3A), and VF: animal score ( $r = 0.39$ ,  $p = 0.0009$ ) (Fig. 3B). The anterior cluster was negatively correlated with insulin levels ( $r = -0.24$ ,  $p = 0.049$ ) and HOMA-IR ( $r = -0.26$ ,  $p = 0.034$ ), and positively with gait speed (DT) ( $r = 0.27$ ,  $p = 0.037$ ) (Fig. 3C) and VF: animal score ( $r = 0.40$ ,  $p = 0.0007$ ) (Fig. 3D).

In the final regression model (corrected for age, hematocrit, hypertension, and GM volume), CBF was negatively associated at both the posterior and anterior clusters with insulin levels ( $r = -0.42$ ,  $p = 0.010$  and  $r = -0.36$ ,  $p = 0.027$ , respectively) and/or HOMA-IR ( $r = -0.35$ ,  $p = 0.038$  and  $r = -0.33$ ,  $p = 0.046$ , respectively) in patients with T2DM. In the control group, CBF was not significantly associated with any of the previously mentioned variables either at the posterior or the anterior cluster. The regional association of baseline CBF with diabetes disease variable, cognitive performance, and mobility performance are summarized in Table 3.

Insulin levels were outside normal range for 4 participants, and these values drove the significant associations observed between baseline CBF and insulin levels and between baseline CBF and HOMA-IR (data not shown). After excluding these participants from

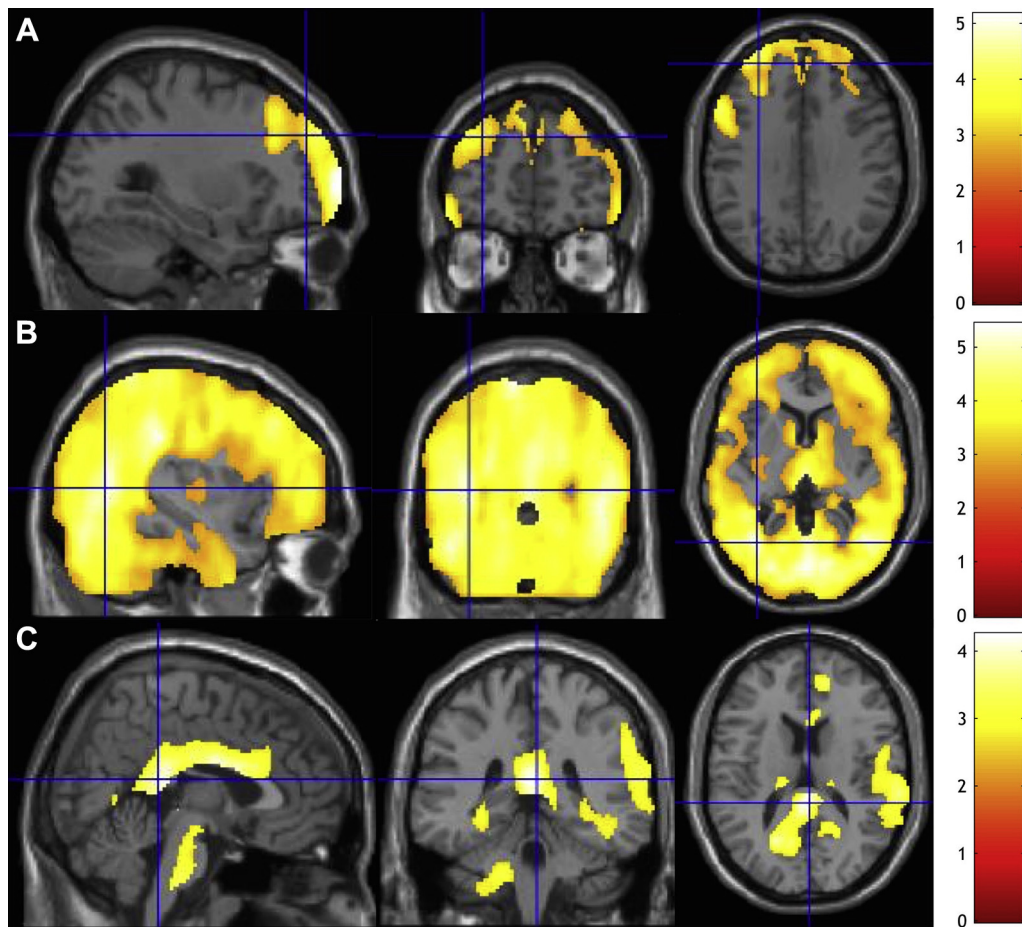


**Fig. 2.** The regions where CBF is significantly associated with (A) age, (B) hematocrit, and (C) hypertension are overlaid on the anatomical brain. CSF was masked out from the regions for better visibility. CBF is reduced significantly in the prefrontal regions as people age. Subjects with higher hematocrit showed significantly decreased CBF in very extensive areas covering almost whole cerebrum, including all frontal, parietal, occipital, and temporal regions. Hypertensive subjects showed significantly increased CBF in the posterior cingulate, anterior cingulate, and prefrontal regions. Abbreviations: CBF, cerebral blood flow; CSF, cerebrospinal fluid.

the analysis, no significant association was observed between baseline CBF and insulin levels and between baseline CBF and HOMA-IR. More subjects are needed to confirm any association between baseline CBF and insulin/HOMA-IR.

After adjusting for age, hematocrit, hypertension, and GM volume, T2DM patients had significantly lower network CBF in DMN ( $p = 0.016$ ), medial visual network ( $p = 0.0063$ ), and cerebellum network ( $p = 0.016$ ) when compared with controls. For all participants, network CBF values at DMN, visual, and cerebellum networks were associated with insulin levels ( $r = -0.31$ ,  $p = 0.0098$ ;  $r = -0.31$ ,  $p = 0.0094$ ; and  $r = -0.30$ ,  $p = 0.012$ , respectively), HOMA-IR ( $r = -0.29$ ,  $p = 0.019$ ;  $r = -0.30$ ,  $p = 0.013$ ; and  $r = -0.29$ ,  $p = 0.018$ , respectively), gait speed (DT) ( $r = 0.32$ ,  $p = 0.012$ ;  $r = 0.37$ ,  $p = 0.0029$ ; and  $r = 0.32$ ,  $p = 0.011$ , respectively), and VF: animal score ( $r = 0.33$ ,  $p = 0.0054$ ;  $r = 0.36$ ,  $p = 0.0027$ ; and  $r = 0.32$ ,  $p = 0.0072$ , respectively). In T2DM participants, network CBF values were negatively associated at DMN, visual, and cerebellum networks with insulin levels ( $r = -0.43$ ,  $p = 0.0079$ ;  $r = -0.40$ ,  $p = 0.015$ ; and  $r = -0.40$ ,  $p = 0.014$ , respectively) and HOMA-IR ( $r = -0.36$ ,  $p = 0.033$ ;  $r = -0.35$ ,  $p = 0.038$ ; and  $r = -0.35$ ,  $p = 0.038$ , respectively). In the control group, network CBF values were not significantly associated with insulin levels and HOMA-IR at either brain network. However, similar to region-based analysis, due to insulin levels outside normal range for 4 participants, more subjects are needed to confirm any association between baseline network CBF and insulin/HOMA-IR.

#### 3.4. CBF at 2-year follow-up and longitudinal CBF change after 2 years

At the 2-year follow-up, we did not observe the significant CBF differences between T2DM patients and controls ( $p > 0.05$ ) at the global level, voxel-by-voxel level, and regional level (for both posterior and anterior regions), after adjusting for age, hematocrit, and hypertension. Longitudinal CBF change from baseline to 2-year follow-up was also not significant at the global, voxel-by-voxel, and/or regional level between the 2 groups, after adjusting for age, hematocrit, and hypertension.

#### 3.5. Correlation of longitudinal CBF change with cognitive and gait changes

For all participants, CBF change at the 2-year follow-up was correlated with the longitudinal change in HVLT: total recall at the posterior cluster ( $r = 0.42$ ,  $p = 0.0095$ ) (Fig. 4A), at the anterior cluster ( $r = 0.36$ ,  $p = 0.029$ ) (Fig. 4B), and at the DMN ( $r = 0.35$ ,  $p = 0.038$ ) (Fig. 4C). One subject experienced very large longitudinal CBF decrease at the posterior cluster, anterior cluster, and DMN (Fig. 4). After removing the subject, the longitudinal CBF change remained significantly associated with the longitudinal change in HVLT: total recall at the posterior cluster, anterior cluster, and DMN ( $r = 0.42$ ,  $p = 0.011$ ;  $r = 0.36$ ,  $p = 0.032$ ; and  $r = 0.35$ ,  $p = 0.038$ , respectively). CBF change at the 2-year follow-up was not

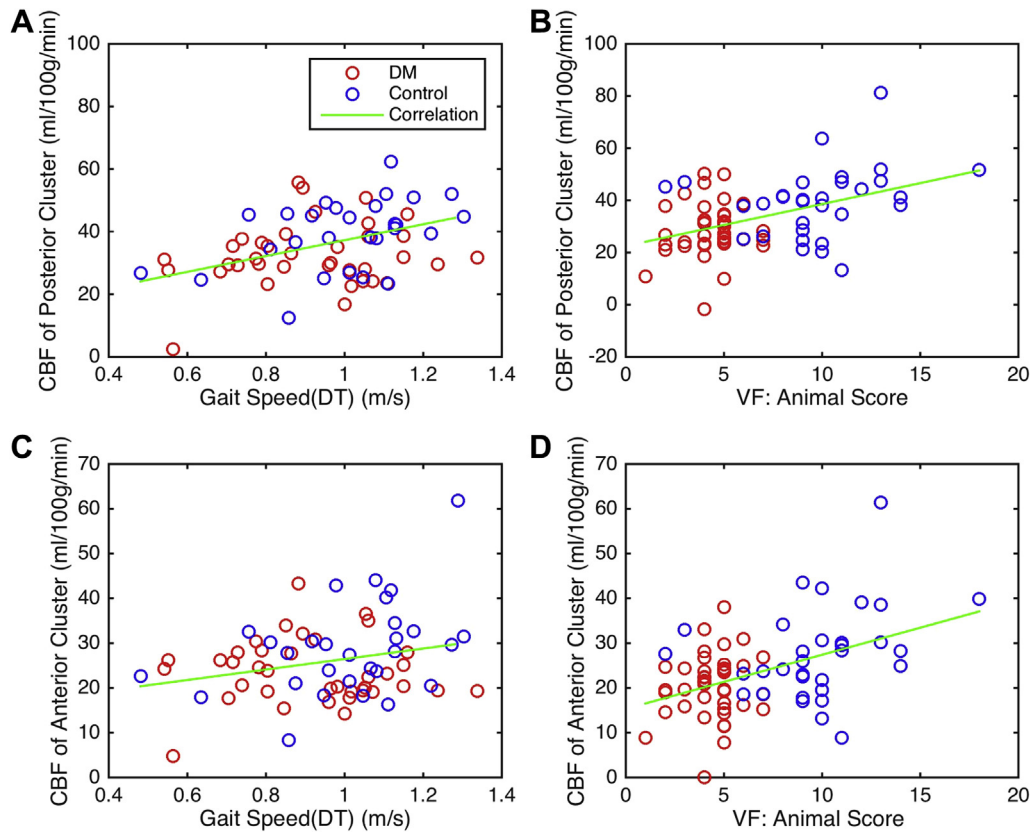


**Fig. 3.** Association of baseline absolute CBF with (A) gait speed (DT) and (B) VF: animal score at the posterior cluster and (C) gait speed (DT) and (D) VF: animal score at the anterior cluster after correcting for age, hematocrit, hypertension, and gray matter volume. Abbreviations: CBF, cerebral blood flow; DT, dual task; VF, verbal fluency.

correlated with either cognitive and gait changes at the visual and cerebellum networks.

In T2DM participants, no significant association was found between CBF change and the change in HVL: total recall either at either cluster or brain network. The regional associations of longitudinal CBF change with longitudinal change of diabetes disease variable, cognitive performance, and mobility performance are summarized (Table 3).

### 3.6. Correlation of longitudinal CBF change with baseline HOMA-IR, cognition

For all participants, the longitudinal CBF decrease at the posterior cluster was significantly associated with greater baseline HOMA-IR values ( $r = -0.36$ ,  $p = 0.031$ ). Similarly, the longitudinal CBF decrease at the anterior cluster and DMN was significantly associated with larger baseline HOMA-IR values ( $r = -0.45$ ,

$p = 0.0063$  and  $r = -0.40$ ,  $p = 0.016$ ) and smaller baseline HVL: Retention ( $r = 0.38$ ,  $p = 0.022$  and  $r = 0.34$ ,  $p = 0.039$ ) (Fig. 5). One subject experienced very large longitudinal CBF decrease at the anterior cluster and DMN (Fig. 5). After removing the subject, the longitudinal CBF decrease remained significantly associated with smaller baseline HVL: Retention at the anterior cluster and DMN ( $r = 0.38$ ,  $p = 0.026$  and  $r = 0.34$ ,  $p = 0.045$ ). The association of longitudinal CBF change with HOMA-IR was mainly influenced by the values of 3 participants that were very high (range: 12–16, while the values from all other subject are in the range of 0–5) (data not shown). After excluding the 3 subjects from the analysis, the association was not significant any more. The relatively lack of subjects with HOMA-IR in the intermediate range (e.g., 5–12) may have contributed to a masked potential association between HOMA-IR and longitudinal CBF change.

For T2DM participants, the longitudinal CBF change at the anterior cluster and DMN was correlated with the baseline HVL:

**Table 3**

Regional association of baseline CBF and longitudinal CBF change with diabetes related variables, cognitive, and mobility measures

	Posterior regions	Anterior regions
Baseline CBF	Baseline insulin <sup>a</sup> ( $r = -0.32$ , $p = 0.0077$ ) Baseline HOMA-IR <sup>a</sup> ( $r = -0.30$ , $p = 0.012$ ) Baseline gait speed (DT) ( $r = 0.38$ , $p = 0.0025$ ) Baseline VF: animal ( $r = 0.39$ , $p = 0.0009$ )	Baseline insulin <sup>a</sup> ( $r = -0.24$ , $p = 0.049$ ) Baseline HOMA-IR <sup>a</sup> ( $r = -0.26$ , $p = 0.034$ ) Baseline gait speed (DT) ( $r = 0.27$ , $p = 0.037$ ) Baseline VF: animal ( $r = 0.40$ , $p = 0.0007$ )
Longitudinal CBF change	Change of HVL: total recall ( $r = 0.42$ , $p = 0.0095$ )	Change of HVL: total recall ( $r = 0.36$ , $p = 0.029$ )
Longitudinal CBF change	Baseline HOMA-IR ( $r = -0.36$ , $p = 0.031$ )	Baseline HOMA-IR ( $r = -0.45$ , $p = 0.0063$ ) Baseline HVL: retention <sup>a</sup> ( $r = 0.38$ , $p = 0.022$ )

Correlation coefficient and  $p$  value for each regional association in the entire study cohort is shown in brackets.

Key: CBF, cerebral blood flow; HOMA-IR, homeostatic model assessment of insulin resistance; HVL, Hopkins Verbal Learning Test; VF, verbal fluency.

<sup>a</sup> Represents significant association in T2DM group.

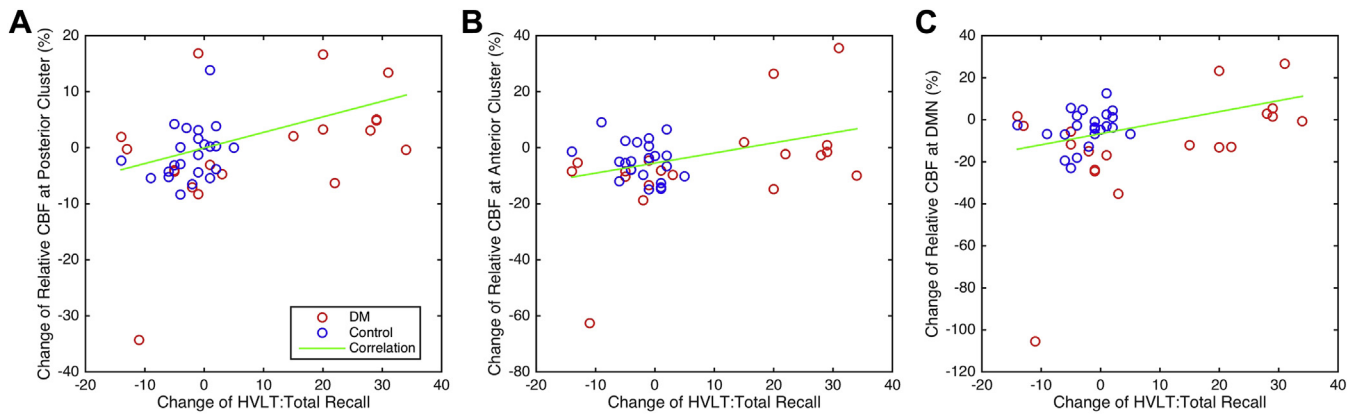


**Fig. 4.** Greater longitudinal decline in CBF at the 2-year follow-up is associated with less total recall in HVLT (A) at the posterior cluster, (B) at the anterior cluster, and (C) at the DMN. Abbreviations: CBF, cerebral blood flow; DMN, default mode network; HVLT, Hopkins Verbal Learning Test.

Retention ( $r = 0.62$ ,  $p = 0.024$  and  $r = 0.60$ ,  $p = 0.024$ , respectively), whereas for the control participants, it was not ( $r = -0.05$ ,  $p = 0.81$  and  $r = -0.035$ ,  $p = 0.89$ , respectively). CBF change at the posterior cluster, visual network, and cerebellum network was not correlated with any baseline variables in either group. The regional associations of the longitudinal CBF change with baseline diabetes disease variable, cognitive performance, and mobility performance are also summarized in Table 3.

#### 4. Discussion

The results of our study have shown that T2DM is associated with impairment of resting CBF in posterior and anterior regions and increased HOMA-IR, as compared with controls matched for age, hypertension, and hematocrit. The pattern of resting CBF impairment is associated with functional (mobility and executive) performance. T2DM patients exhibit significantly reduced CBF in the medial visual network, cerebellum network, and DMN, which include one posterior cluster in the occipital, cerebellum, posterior cingulate, precuneus, thalamus, parietotemporal, basal ganglia regions, and one anterior cluster in the prefrontal region of the DMN. Reduced CBF was strongly correlated with higher hematocrit globally. These findings are independent of the presence of hypertension and age. In addition, reduced CBF was also associated with

baseline memory performance and insulin resistance, and with compromised gait, lower memory and executive function scores at the 2-year follow-up.

The association of T2DM with CBF has been investigated in several studies, using a variety of techniques, including positron emission tomography, single-photon emission computed tomography, and ASL. The results did not reach an agreement yet. Some studies have reported decreased CBF in T2DM (Last et al., 2007; Nagamachi et al., 1994; Novak et al., 2006; Xia et al., 2015), whereas others did not observe CBF alteration in T2DM (Novak et al., 2011; Rusinek et al., 2015; Tiehuis et al., 2008). Most of the studies reporting no CBF alteration in T2DM typically used large regions of interest and/or did not adequately account for the potential risk factors. The regions of interest were chosen as the entire brain, whole GM, or several large cortical regions. Regarding the risk factors, some studies did not account for any hypertension effect, although hypertension has been reported more frequent in T2DM than in nondiabetic populations (Colosia et al., 2013). The higher frequency of hypertension in T2DM has been observed in the present study. Some studies did not have similar gender distributions between T2DM and nondiabetic control groups, but female subjects had higher CBF than male subjects (Cur and Gur, 1990; Pirson et al., 2006), which may obscure the CBF difference between the groups. Some studies also did not account for brain

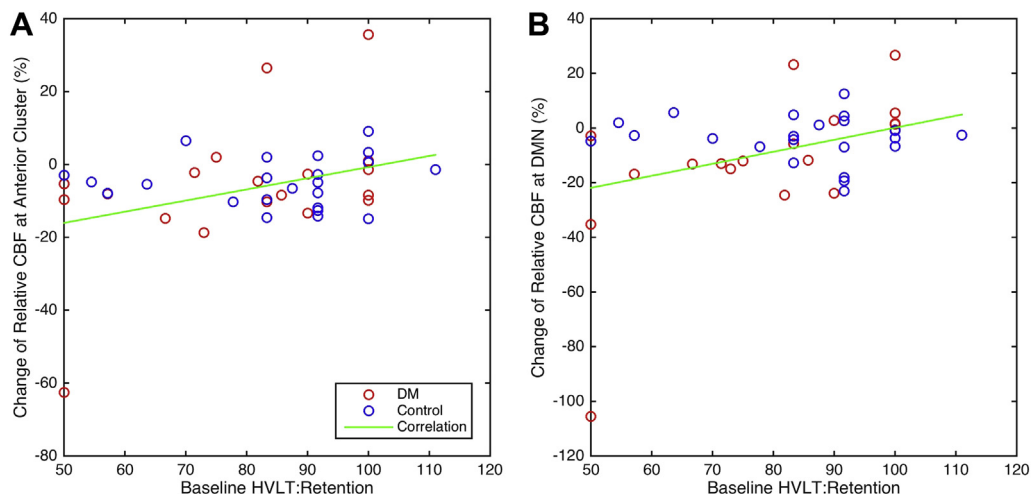


**Fig. 5.** Greater longitudinal decline in CBF after 2-year follow-up (A) at the anterior cluster and (B) at the DMN is associated with reduced baseline HVLT: retention. Abbreviations: CBF, cerebral blood flow; DMN, default mode network; HVLT, Hopkins Verbal Learning Test.

volume difference, which has been shown to largely explain reduced CBF (Sabri et al., 2000).

We observed decreased CBF in T2DM, mainly in visual network, cerebellum network, and DMN regions after correcting for age, hematocrit (or gender), hypertension, and GM volume. This is consistent with our previous findings that T2DM reduces CBF velocity and regional cerebral vasoreactivity of CO<sub>2</sub> challenges in the parietal and occipital regions (Novak et al., 2006). Our findings are consistent with a recent T2DM ASL-CBF study (Xia et al., 2015). They reported that the main effects of T2DM were primarily in visual network and DMN regions. We found an additional cerebellum region affected by T2DM. Presumably, the additional regions observed may emerge from the more sensitive ASL MRI sequence for our CBF measurements. The PCASL sequence that was used in our study has been recommended as the most effective noninvasive CBF measurement in clinical practice (Alsop et al., 2014). More importantly, we have shown that HOMA-IR is a potential predictor of CBF decline at the 2-year follow-up period.

We observed that age, hematocrit, and hypertension alter CBF in different regions. This indicates that correction for these factors is crucial, especially when comparing CBF in different brain regions. Older age and higher hematocrit were associated with decreased CBF in the present study, whereas hypertension was associated with regionally increased CBF. In fact, the inverse relationship between hematocrit and global CBF has been noted in earlier studies using microsphere techniques (Hudak et al., 1986; Massik et al., 1987; Thomas et al., 1977) and Xe-133 CT methods (Kusunoki et al., 1981). We have shown the inverse correlation between hematocrit and almost entire brain cerebrum, which is in line with the earlier results. The underlying reasons for the relationship are not clear from our study alone. The possible explanations could include 2 perspectives: (1) low hematocrit leads to reduced oxygen supply, and thus results in increased blood flow because of brain autoregulation and (2) low hematocrit leads to reduced viscosity and further increases blood flow velocity. We have observed significantly higher CBF in female participants compared with male participants (results not shown), which could be resulted from the lower hematocrit in women than men. We have found that hypertension is associated with increased CBF both globally and locally. Noticing that most hypertensive participants in our study were under antihypertensive treatment, the findings are in agreement with the literature. Reduction of BP in older populations has been associated with increased CBF and blood flow velocity (Lipsitz et al., 2005).

In the T2DM group, impaired CBF at the baseline was associated with higher insulin level and HOMA-IR, but not with worse performance in mobility and executive function. Interestingly, greater CBF was correlated with faster walking and better executive function (VF: animal scores) in the entire study cohort. These results may be due to the range of variables and/or the small sample size of mobility and executive function in each group. We found correlation between CBF and mobility function and between CBF and executive function, once we included the entire population in the analyses (with broader range and/or the larger sample size). However, whether significant association was found with T2DM group specifically, it is important to point out that reduced CBF may exacerbate the deficits in executive function and the mobility function in older adults.

The T2DM-specific pattern of reduced CBF (in posterior and anterior regions) is very similar to the pattern observed in patients with mild cognitive impairment (MCI) and Alzheimer's disease (AD) (Li et al., 2016; Mevel et al., 2011). Moreover, in the present study, the T2DM-specific pattern of reduction in CBF was associated with insulin resistance, mobility function, and executive function. The association was independent of age, hematocrit (or gender),

hypertension, and brain volume. Note that the severity of AD is mostly assessed based on status of cognitive and executive function (especially categorical VF test such as name of animals). Our participants received careful neuropsychological assessment and were not cognitively impaired according to the current criteria for MCI. These results could indicate that insulin resistance may be a marker of AD that is associated with reduced CBF, and cognitive and executive impairment before the onset of MCI. These findings suggest that the amelioration of insulin resistance in people in high risk of developing T2DM (e.g., impaired glucose metabolism) could be a way to prevent them from developing cognitive or mobility impairment.

The longitudinal design of the study allows us to estimate the relationships among the studied variables and shed light on the potential causal effect of insulin resistance on T2DM progression and severity. We observed that the longitudinal CBF change was associated with baseline HOMA-IR in the entire cohort, but not in the T2DM and control groups separately. This might be attributed to a reduced power to detect such associations in the separate groups, due to the reduced sample size at the 2-year follow-up. These results indicate that insulin resistance in T2DM is related to longitudinal CBF change. Our findings suggest that the longitudinal change in CBF might represent modulation of brain function by insulin resistance.

No difference in CBF at the 2-year follow-up was observed between the T2DM patients and controls, possibly due to the increased variance in T2DM group secondary to the reduced sample size. However, we observed that the longitudinal CBF decrease was associated with the decline in memory (HVLT: total recall) function. This demonstrates that CBF decrease can be indicative of cognitive decline as T2DM progresses. We have identified that the baseline HOMA-IR can predict longitudinal decrease of CBF. Taken together, these results suggest that controlling insulin resistance may potentially prevent further cognitive decline in T2DM and that insulin resistance may be a common pathway between T2DM, AD, and other dementias.

Our study shed light on the adverse effects of insulin resistance to the longitudinal CBF change in T2DM. The reduced sample size in the 2-year follow-up and the reduced power associated with this might have affected our ability to detect existing associations between T2DM, CBF, and cognitive/mobility performance or the changes between these variables at the follow-up period; therefore, the overall impact of diabetes on CBF and cognitive/mobility performance may be even greater. Interestingly, we also provide evidence that T2DM is associated with a pattern of reduced CBF in the DMN, visual, and cerebellum networks, and that the pattern of resting CBF impairment is closely related to the decline of memory, executive, and mobility functions. However, resting CBF was not found associating with either fasting blood glucose or HbA1c. The pathways by which insulin resistance may affect brain perfusion and cognition are independent of glycemic control and require further investigation. A study with larger sample size and longer follow-up is warranted to confirm the association of HOMA-IR and longitudinal CBF decrease in T2DM.

#### Disclosure statement

The authors do not have any conflicts of interest. Appropriate approval and procedures were used concerning human subjects.

#### Acknowledgements

The study was supported by NIH-NIA 1R01-AG0287601A2, NIH-NIDDK 5R21 DK084463, NIH-NIDDK 1R01DK13902-01A1, American Diabetes Association, Clinical 1-03-CR-23, and 1-06-CR-25 to Dr Novak. The project described was supported by grant number

UL1 RR025758- Harvard Clinical and Translational Science Center and M01-RR-01032, from the National Center for Research Resources.

## References

- Alsop, D.C., Detre, J.A., 1996. Reduced transit-time sensitivity in noninvasive magnetic resonance imaging of human cerebral blood flow. *J. Cereb. Blood Flow Metab.* 16, 1236–1249.
- Alsop, D.C., Detre, J.A., Golay, X., Gunther, M., Hendrikse, J., Hernandez-Garcia, L., Lu, H., Macintosh, B.J., Parkes, L.M., Smits, M., van Osch, M.J., Wang, D.J., Wong, E.C., Zaharchuk, G., 2014. Recommended implementation of arterial spin-labeled perfusion MRI for clinical applications: a consensus of the ISMRM perfusion study group and the European consortium for ASL in dementia. *Magn. Reson. Med.* 73, 102–116.
- Ashburner, J., Friston, K.J., 2005. Unified segmentation. *Neuroimage* 26, 839–851.
- Benton, A.L., Hamsher, K., 1989. *Multilingual Aphasia Examination*. Manual of Instructions, second ed. AJA Associates, Iowa City.
- Brownlee, M., 2005. The pathobiology of diabetic complications: a unifying mechanism. *Diabetes* 54, 1615–1625.
- Buxton, R.B., Frank, L.R., Wong, E.C., Siewert, B., Warach, S., Edelman, R.R., 1998. A general kinetic model for quantitative perfusion imaging with arterial spin labeling. *Magn. Reson. Med.* 40, 383–396.
- Chung, C.C., Pimentel, D., Jordan, A.J., Hao, Y., Milberg, W., Novak, V., 2015. Inflammation-associated declines in cerebral vasoreactivity and cognition in type 2 diabetes. *Neurology* 85, 450–458.
- Colosia, A.D., Palencia, R., Khan, S., 2013. Prevalence of hypertension and obesity in patients with type 2 diabetes mellitus in observational studies: a systematic literature review. *Diabetes Metab. Syndr. Obes.* 6, 327–338.
- Dai, W., Garcia, D., de Bazelaire, C., Alsop, D.C., 2008. Continuous flow-driven inversion for arterial spin labeling using pulsed radio frequency and gradient fields. *Magn. Reson. Med.* 60, 1488–1497.
- Dai, W., Varma, G., Scheidegger, R., Alsop, D.C., 2016. Quantifying fluctuations of resting state networks using arterial spin labeling perfusion MRI. *J. Cereb. Blood Flow Metab.* 36, 463–473.
- Detre, J.A., Leigh, J.S., Williams, D.S., Koretsky, A.P., 1992. Perfusion imaging. *Magn. Reson. Med.* 23, 37–45.
- Eklund, A., Nichols, T.E., Knutsson, H., 2016. Cluster failure: why fMRI inferences for spatial extent have inflated false-positive rates. *Proc. Natl. Acad. Sci. U. S. A.* 113, 7900–7905.
- Folstein, M.F., Folstein, S.E., McHugh, P.R., 1975. "Mini-mental state". A practical method for grading the cognitive state of patients for the clinician. *J. Psychiatr. Res.* 12, 189–198.
- Franke, K., Gaser, C., Manor, B., Novak, V., 2013. Advanced BrainAGE in older adults with type 2 diabetes mellitus. *Front. Aging Neurosci.* 5, 90.
- Grande, L.J., Milberg, W., Rudolph, J., Gaziano, M., McGlinchey, R., 2005. A timely screening for executive functions and memory. *J. Int. Neuropsychol. Soc.* 11, 31.
- Gur, R.E., Gur, R.C., 1990. Gender differences in regional cerebral blood flow. *Schizophr. Bull.* 16, 247–254.
- Henriksen, O.M., Jensen, L.T., Krabbe, K., Guldberg, P., Teerlink, T., Rostrup, E., 2014. Resting brain perfusion and selected vascular risk factors in healthy elderly subjects. *PLoS One* 9, e97363.
- Henriksen, O.M., Kruuse, C., Olesen, J., Jensen, L.T., Larsson, H.B., Birk, S., Hansen, J.M., Wienecke, T., Rostrup, E., 2013. Sources of variability of resting cerebral blood flow in healthy subjects: a study using  $(1/3)(3)\text{Xe}$  SPECT measurements. *J. Cereb. Blood Flow Metab.* 33, 787–792.
- Hudak, M.L., Koehler, R.C., Rosenberg, A.A., Traystman, R.J., Jones Jr., M.D., 1986. Effect of hemocrit on cerebral blood flow. *Am. J. Physiol.* 251, H63–H70.
- Kim, J.A., Montagnani, M., Koh, K.K., Quon, M.J., 2006. Reciprocal relationships between insulin resistance and endothelial dysfunction: molecular and pathophysiological mechanisms. *Circulation* 113, 1888–1904.
- Klein, A., Andersson, J., Ardekani, B.A., Ashburner, J., Avants, B., Chiang, M.C., Christensen, G.E., Collins, D.L., Gee, J., Hellier, P., Song, J.H., Jenkinson, M., Lepage, C., Rueckert, D., Thompson, P., Vercauteren, T., Woods, R.P., Mann, J.J., Parsey, R.V., 2009. Evaluation of 14 nonlinear deformation algorithms applied to human brain MRI registration. *Neuroimage* 46, 786–802.
- Kusunoki, M., Kimura, K., Nakamura, M., Isaka, Y., Yoneda, S., Abe, H., 1981. Effects of hematocrit variations on cerebral blood flow and oxygen transport in ischemic cerebrovascular disease. *J. Cereb. Blood Flow Metab.* 1, 413–417.
- Last, D., Alsop, D.C., Abduljalil, A.M., Marquis, R.P., de Bazelaire, C., Hu, K., Cavallerano, J., Novak, V., 2007. Global and regional effects of type 2 diabetes on brain tissue volumes and cerebral vasoreactivity. *Diabetes Care* 30, 1193–1199.
- Li, Y., Wang, X., Li, Y., Sun, Y., Sheng, C., Li, H., Li, X., Yu, Y., Chen, G., Hu, X., Jing, B., Wang, D., Li, K., Jessen, F., Xia, M., Han, Y., 2016. Abnormal resting-state functional connectivity strength in mild cognitive impairment and its conversion to Alzheimer's disease. *Neural Plast.* 2016, 4680972.
- Lipsitz, L.A., Gagnon, M., Vyas, M., Iloputaife, I., Kiely, D.K., Sorond, F., Serrador, J., Cheng, D.M., Babikian, V., Cupples, L.A., 2005. Antihypertensive therapy increases cerebral blood flow and carotid distensibility in hypertensive elderly subjects. *Hypertension* 45, 216–221.
- Liu, Y., Zhu, X., Feinberg, D., Guenther, M., Gregori, J., Weiner, M.W., Schuff, N., 2012. Arterial spin labeling MRI study of age and gender effects on brain perfusion hemodynamics. *Magn. Reson. Med.* 68, 912–922.
- Massik, J., Tang, Y.L., Hudak, M.L., Koehler, R.C., Traystman, R.J., Jones Jr., M.D., 1987. Effect of hematocrit on cerebral blood flow with induced polycythemia. *J. Appl. Physiol.* (1985) 62, 1090–1096.
- Matthews, D.R., Hosker, J.P., Rudenski, A.S., Naylor, B.A., Treacher, D.F., Turner, R.C., 1985. Homeostasis model assessment: insulin resistance and beta-cell function from fasting plasma glucose and insulin concentrations in man. *Diabetologia* 28, 412–419.
- Mevel, K., Chetelat, G., Eustache, F., Desgranges, B., 2011. The default mode network in healthy aging and Alzheimer's disease. *Int. J. Alzheimers Dis.* 2011, 535816.
- Mogi, M., Horiuchi, M., 2011. Neurovascular coupling in cognitive impairment associated with diabetes mellitus. *Circ. J.* 75, 1042–1048.
- Nagamachi, S., Nishikawa, T., Ono, S., Ageta, M., Matsuo, T., Jinouchi, S., Hoshi, H., Ohnishi, T., Futami, S., Watanabe, K., 1994. Regional cerebral blood flow in diabetic patients: evaluation by N-isopropyl-123I-IMP with SPECT. *Nucl. Med. Commun.* 15, 455–460.
- Novak, V., Last, D., Alsop, D.C., Abduljalil, A.M., Hu, K., Lepicovsky, L., Cavallerano, J., Lipsitz, L.A., 2006. Cerebral blood flow velocity and periventricular white matter hyperintensities in type 2 diabetes. *Diabetes Care* 29, 1529–1534.
- Novak, V., Zhao, P., Manor, B., Sejdic, E., Alsop, D., Abduljalil, A., Roberson, P.K., Munshi, M., Novak, P., 2011. Adhesion molecules, altered vasoreactivity, and brain atrophy in type 2 diabetes. *Diabetes Care* 34, 2438–2441.
- Pirson, A.S., Vander Borgh, T., Van Laere, K., 2006. Age and gender effects on normal regional cerebral blood flow. *AJNR Am. J. Neuroradiol.* 27, 1161–1162. author reply 62–63.
- Pugh, K.G., Kiely, D.K., Milberg, W.P., Lipsitz, L.A., 2003. Selective impairment of frontal-executive cognitive function in African Americans with cardiovascular risk factors. *J. Am. Geriatr. Soc.* 51, 1439–1444.
- Roberts, R.O., Knopman, D.S., Cha, R.H., Mielke, M.M., Pankratz, V.S., Boeve, B.F., Kantarci, K., Geda, Y.E., Jack Jr., C.R., Petersen, R.C., Lowe, V.J., 2014. Diabetes and elevated hemoglobin A1c levels are associated with brain hypometabolism but not amyloid accumulation. *J. Nucl. Med.* 55, 759–764.
- Rusinek, H., Ha, J., Yau, P.L., Storey, P., Tarsi, A., Tsui, W.H., Frosch, O., Azova, S., Convit, A., 2015. Cerebral perfusion in insulin resistance and type 2 diabetes. *J. Cereb. Blood Flow Metab.* 35, 95–102.
- Sabri, O., Hellwig, D., Schreckenberger, M., Schneider, R., Kaiser, H.J., Wagenknecht, G., Mull, M., Buell, U., 2000. Influence of diabetes mellitus on regional cerebral glucose metabolism and regional cerebral blood flow. *Nucl. Med. Commun.* 21, 19–29.
- Shapiro, A.M., Benedict, R.H., Schretlen, D., Brandt, J., 1999. Construct and concurrent validity of the Hopkins verbal learning test-revised. *Clin. Neuropsychol.* 13, 348–358.
- Starr, J.M., Wardlaw, J., Ferguson, K., MacLulich, A., Deary, I.J., Marshall, I., 2003. Increased blood-brain barrier permeability in type II diabetes demonstrated by gadolinium magnetic resonance imaging. *J. Neurol. Neurosurg. Psychiatry* 74, 70–76.
- Thomas, D.J., Marshall, J., Russell, R.W., Wetherley-Mein, G., du Boulay, G.H., Pearson, T.C., Symon, L., Zilkha, E., 1977. Effect of haematocrit on cerebral blood-flow in man. *Lancet* 2, 941–943.
- Tiehuis, A.M., Vincken, K.L., van den Berg, E., Hendrikse, J., Manschot, S.M., Mali, W.P., Kappelle, L.J., Biessels, G.J., 2008. Cerebral perfusion in relation to cognitive function and type 2 diabetes. *Diabetologia* 51, 1321–1326.
- Umegaki, H., 2014. Type 2 diabetes as a risk factor for cognitive impairment: current insights. *Clin. Interv. Aging* 9, 1011–1019.
- van Elderen, S.G., de Roos, A., de Craen, A.J., Westendorp, R.G., Blauw, G.J., Jukema, J.W., Bollen, E.L., Middelkoop, H.A., van Buchem, M.A., van der Grond, J., 2010. Progression of brain atrophy and cognitive decline in diabetes mellitus: a 3-year follow-up. *Neurology* 75, 997–1002.
- Wang, J., Alsop, D.C., Li, L., Listerud, J., Gonzalez-At, J.B., Schnall, M.D., Detre, J.A., 2002. Comparison of quantitative perfusion imaging using arterial spin labeling at 1.5 and 4.0 Tesla. *Magn. Reson. Med.* 48, 242–254.
- Wechsler, D., 1987. *Wechsler Memory Scale-Revised (Manual)*. Psychological Corporation, New York.
- Williams, D.S., Detre, J.A., Leigh, J.S., Koretsky, A.P., 1992. Magnetic resonance imaging of perfusion using spin inversion of arterial water. *Proc. Natl. Acad. Sci. U. S. A.* 89, 212–216.
- Wong, R.H., Scholey, A., Howe, P.R., 2014. Assessing premorbid cognitive ability in adults with type 2 diabetes mellitus—a review with implications for future intervention studies. *Curr. Diab. Rep.* 14, 547.
- Woo, C.W., Krishnan, A., Wager, T.D., 2014. Cluster-extent based thresholding in fMRI analyses: pitfalls and recommendations. *Neuroimage* 91, 412–419.
- Wu, W.C., Fernandez-Seara, M., Detre, J.A., Wehrli, F.W., Wang, J., 2007. A theoretical and experimental investigation of the tagging efficiency of pseudocontinuous arterial spin labeling. *Magn. Reson. Med.* 58, 1020–1027.
- Xia, W., Rao, H., Spaeth, A.M., Huang, R., Tian, S., Cai, R., Sun, J., Wang, S., 2015. Blood pressure is associated with cerebral blood flow alterations in patients with T2DM as revealed by perfusion functional MRI. *Medicine* 94, e2231.
- Xu, G., Rowley, H.A., Wu, G., Alsop, D.C., Shankaranarayanan, A., Dowling, M., Christian, B.T., Oakes, T.R., Johnson, S.C., 2010. Reliability and precision of pseudo-continuous arterial spin labeling perfusion MRI on 3.0 T and comparison with 15O-water PET in elderly subjects at risk for Alzheimer's disease. *NMR Biomed.* 23, 286–293.
- Zhou, H., Zhang, X., Lu, J., 2014. Progress on diabetic cerebrovascular diseases. *Bosn. J. Basic Med. Sci.* 14, 185–190.